DOI: https://doi.org/10.46354/i3m.2019.imaaca.006

BOND GRAPHS BASED FORMATION CONTROL OF HOLONOMIC ROBOTS

Matías Nacusse [(a)], Martín Crespo [(a,b)], Sergio Junco [(a)]

[(a)] Laboratorio de Automatización y Control (LAC), Departamento de Control, FCEIA, UNR. Rosario, Argentina
[(b)] CONICET: Consejo Nacional de Investigaciones Científicas y Técnicas. Argentina

[(a)]nacusse@fceia.unr.edu.ar, crespom@fceia.unr.edu.ar, sjunco@fceia.unr.edu.ar

ABSTRACT

This paper tackles the problem of formation control for a group of holonomic vehicles using the Bond Graphs formalism. The control law design follows an energy based approach in which the agents are connected each other by means of virtual springs and dampers. The obtained control law is then robustified using a disturbance observer. The properties are studied in the port Hamiltonian (pH) formalism which allows to show that the resulting closed-loop system is l_2 *weakly string stable* with respect to disturbances. The desired behavior of the closed-loop system is illustrated with some numerical simulation experiments.

Keywords: Formation Control, Bond Graph, Port Hamiltonian System, Interconnection and Damping assignment, Robust Control.

1. INTRODUCTION

The coordinated control of autonomous robots is an important area of research and its field of application is broad, encompassing problems such as Formation Control, sensor deployment (Tuna, Gungor and Gulez, 2014), map generation and capture (Tuna, Gungor and Gulez, 2014), (Tuna, Güngör and Potirakis, 2015), performing search and rescue tasks of people in hazard environments (Ollero et al., 2007), building monitoring and surveillance (Feddema, Lewis and Schoenwald, 2002), ground cleaning (Galceran and Carreras, 2013), lawn mowing (Yuming et al., 2011), crops harvesting (Ji et al., 2014), and ground mineral deposits detecting (Hameed, 2014), etc.

This paper tackles the problem of Formation Control (FC) (Soni and Hu, 2018) for a group of holonomic vehicles, which are represented as point masses in the plane. This group of vehicles, or platoon, moves at the same speed maintaining a desired geometry, which is specified by a desired inter-vehicle space.

A common and no desirable effect of these kind of systems is the *accordion* effect or *string instability* (Swaroop and Hedrick, 1996) (Swaroop and Hedrick, 1999). This effect takes place when the fluctuation of the speed of one vehicle, caused by a variable speed of the leader for example or by the action of external disturbances acting on the vehicles, propagates through the network increasing the distance among the vehicles especially downstream. These problems were well treated in the literature with multiple approaches, depending on the sensing capabilities of each agents and the desired topology, to mention: the *Leader-follower* approach (Gao et al., 2018), where each agent has the knowledge of the position and velocity of the leader, i.e. the leader must broadcast its position, velocity and, possibly, its acceleration in a speed tracking configuration, to all its followers. This methodology has two main drawbacks which are the lack of inter-vehicle information feedback throughout the group which can cause collisions among agents and the fact that the loss of leader information causes a fail on the entire group. Another methodology that requires less demand from the communication network is the *Predecessor-Following* approach (Knorn and Middleton, 2013) approach, where each agent has the knowledge of the relative position and velocity only of its predecessor agent. In (Seiler, Pant and Hedrick, 2004) the authors demonstrates that this configuration is always string unstable measuring only the relative position of the agents. Another approach that results as the combination of the previous two is the Leader-Predecessor-Following (Xiao, Gao and Wang, 2009) and guaranties string stability demanding more requirements to the communication network or other approaches that uses the information of the relative velocity and acceleration among the agents. The Predecessor-Successor approach or also known as *Bidirectional topology*, in which the control law of each agent is defined by the information of its Predecessors-Successors agents, i.e. the information propagates both upstream and downstream in the platoon. In (Barooah, Mehta and Hespanha, 2009) and (Seiler, Pant and Hedrick, 2004) it is shown that linear symmetric and bidirectional string measuring only the relative position of the agents is string unstable. The reader must refer to (Soni and Hu, 2018), (Zheng et al., 2016), (Middleton and Braslavsky, 2010), (Knorn and Middleton, 2013) for a sound review of these topologies and others.

The problem of FC can be attacked using a centralized or a decentralized approach. The first one demands the use of a global communication network that allows the exchange of information among vehicles and the computation of each control law. While, in the second approach, each agent computes its local control law using only local information, i.e. the i^{th} vehicle receives information only from its neighbor vehicles. The main goal in this work is to solve the FC problem using only local information, i.e. the i^{th} vehicle receives information only from its neighbor vehicles, rather than centralized controllers (Arcak, 2007), this reduces the requirements of the communication network to onboard sensors like radars, and the interconnection structure among the agents is closely related to the way that an agent acquires and process the information of its surrounding agents. To that end the desired behavior of the group pursued in this work, which is physically inspired, consists in a network of N masses coupled by virtual spring and dampers in parallel where the effect of these virtual elements is bidirectional. Different configurations between vehicle couplings are considered, from the weakly coupled configuration to the strongly or fully coupled. Due to direct connection with physics, the Bond Graph (BG) (Karnopp, Margolis and Rosenberg, 2006) formalism is used as a tool for network modeling and control law design.

The control law design follows an energy based approach, of the kind of interconnection and damping assignment (IDA-PBC) (Ortega and García-Canseco, 2004), completely designed in the BG domain (Junco, 2004) where: first, the closed-loop specifications are expressed by a so-called Target Bond Graph (TBG) representing the equivalent closed-loop behavior of the network. Then, in order to obtain the control law, the controlled sources –which provide the manipulated variables in the BG model of the plant– are prototyped (meaning that their behavior is expressed through BG components) in such a way that their power-interconnection with the rest of the plant BG –which is called a Virtual BG (VBG)– matches the TBG. Finally, the control law is obtained from the VBG by simply reading the outputs of the prototyped sources with the help of the causal assignment in the VBG.

To make the control law robust against external disturbances and the controlled system string stable with respect to input bounded disturbances, an extra control law based in the construction of a disturbance observer (DO) (Radke and Gao, 2006) is added.

The DBG was proposed by (Samantaray et al., 2006) for numerical evaluation of analytical redundant relationships. These are calculated to perform fault detection and isolation in an active fault tolerant control framework. Here the analytical redundant relationships or residues obtained from a closed-loop DBG are used to robustify the control law. The closed-loop DBG has been used to robustify control law against modelling error, parameter dispersion and external disturbances that acts in the same channel as the control input in (Nacusse and Junco, 2011) and (Nacusse and Junco, 2015). Recently, in (Nacusse, Donaire and Junco, 2018), this approach was formalized and extended, for disturbances with relative degree greater than one, in the pH framework with the form of DO.

The paper is organized as follows: Section 2 formulates the problem to be solved. Section 3 presents some tools and the metholodogy to be used. Section 4 presents the major result of the paper. Finally, in Section 5, some simulation results are provided to show the good performance of the control system.

2. PROBLEM FORMULATION

In this work a group of N of holonomic vehicles moving in a workspace $W \subset \mathbb{R}^2$ is considered. This group of vehicles, or platoon, moves at the same speed maintaining a desired geometry which is specified by a desired inter-vehicle space.

The equation of motion of each vehicle or agent is described by the double integrator, i.e. $\ddot{q}_i = u_i$ (with $i = 0, \dots, N$), being $q_i \in \mathbb{R}^2$the position of the i^{th} agent and $u_i = [u_{xi} \quad u_{yi}]^T$ the control input, and represented in the pH framework as in (1), being $q_i = [x_i \quad y_i]^T \in \mathbb{R}^2$ the Cartesian position of the i^{th} agent and $p_i = m_i[\dot{x}_i \quad \dot{y}_i]^T \in \mathbb{R}^2$ the linear momentum of the i^{th} point mass.

$$\begin{gathered}\begin{bmatrix}\dot{q}_i\\ \dot{p}_i\end{bmatrix} = \begin{bmatrix}0_2 & I_2\\ -1_2 & 0_2\end{bmatrix}\begin{bmatrix}\nabla_q H\\ \nabla_p H\end{bmatrix} + \begin{bmatrix}0_2\\ 1_2\end{bmatrix}(u_i + d_i)\\ y = \nabla_p H\end{gathered} \tag{1}$$

Where 0_2 and I_2 are the $2x2$ zero and identity matrices respectively. $H(q_i, p_i) = \frac{1}{2} p_i^T M_i^{-1} p_i$ is the storage function, $\nabla_q H = \partial H/\partial q$, $\nabla_p H = \partial H/\partial p$, $M_i = diag(m_i, m_i)$, $d_i = d_{ci} + d_{di}(t)$ is the perturbation input, where $d_i = [d_{xi} \quad d_{yi}]^T$, $d_{ci} = cte$ and $d_d(t)$ is bounded and variable with respect to time.

The FC Problem can be tackled using a centralized or a decentralized approach. The first one demands the use of a global communication network that allows the exchange of information among vehicles and the computation of each control law. In the second approach, each agent computes its local control law using only local information, i.e. the i^{th} vehicle receives information only from its neighbor vehicles. This work is framed in this last approach defining a physically inspired behavior of the group which consists in a network of N masses coupled by virtual springs and dampers in parallel. The connection among agents is bidirectional except for the leader which has its own control law independent of the other agents.

Two agents that are closer than a distance D_i are considered *neighbors* and have access to relative information. Being n_i the number of agents inside the *neighborhood*, each agent is connected to other and the number of coupling is indicated through a coupling index $k_i = \{1, 2, \dots n_i\}$, which is defined as the number of bidirectional couplings. From the aforementioned, the following definitions are given.

Definition 1: the i^{th} agent is said to be a *Fully Coupled Agent* with distance D_i if its coupling index is $k_i = n_i$.

Definition 2: the i^{th} agent is said to be a *Partially Coupled Agent* with distance D_i and index k_i if its coupling index is equal to $k_i = n < n_i$.

Definition 3: a network with N agents is said to be a *Fully Coupled Network* with distance D_i if all its agents are fully coupled agents, otherwise is a *Partially Coupled Network.*

Figure 1 shows, without loss of generality, an array of $N = 25$ equally-spaced agents, where the i^{th} agent defines its *neighborhood* with a distance $D_i = 1.5$. The *neighborhood* it is composed by eight agents, i.e. $n_i = 8$, which are represented, in Figure 1, as the black dots inside the dashed circle. Notice that, if the i^{th} agent is a *partially coupled agent* then there are several coupling combinations among the i^{th} agent and its *neighbors* inside the dotted circle.

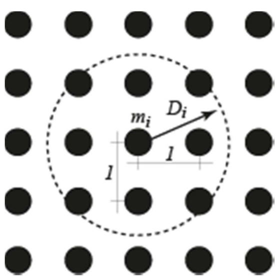

Figure 1: Definition of the *neighbourhood* of the i^{th} agent

The definition of string stability with respect to disturbances presented in (Knorn et al., 2014) will be used.

Definition 4: Consider a system described by $\dot{x} = f(x, d)$ with states $x \in R^{4N}$ and disturbances $d \in R^{2N}$, $f \in R^{4N}$ satisfying $f(x^*, 0) = 0$, where $m$is the number of springs. The equilibrium x^* is l_2 *weakly string stable with respect to disturbances* $d(t)$, if given any $\epsilon > 0$, there exists $\delta_1(\epsilon) > 0$ and $\delta_2(\epsilon) > 0$ (independent of N) such that:

$$|x(0) - x^*| < \delta_1(\epsilon) \; and \; \| d(.) \|_2 < \delta_2(\epsilon) \qquad (2)$$

implies

$$\|x(t) - x^*\|_\infty = sup_{t\geq 0}|x(t) - x^*| < \epsilon \; \forall N \geq 1 \quad (3)$$

Where $\| d(.) \|_2 = \sqrt{\int_0^\infty |d(t)|^2 dt}$

3. BACKGROUND AND METHODOLOGY

In this section the methodology used in the paper is detailed through a simple example consisting in two agents interconnected by means of physical components, namely a spring and a damper.

In the sequel it is assumed that the control signal has the form $u = u_{IDA} + v$, where u_{IDA} is an IDA-PBC law designed for the unperturbed system, i.e. (1) with $d = 0$, and v is an extra control input obtained from a DO.

The methodology employed can be summarized as follows: First and IDA-PBC strategy in the BG domain, using the virtual prototyping method (Junco, 2004), is employed to define the control law in absence of disturbance, i.e. $d = 0$. Then, the closed loop system equations in the pH framework are obtained from the BG domain using the methodology developed in (Donaire and Junco, 2009). Finally, the previous closed loop system is robustified using the output of a DO in the pH framework (Nacusse, Donaire and Junco, 2018).

3.1. IDA-PBC in the BG domain

The design of the control law u follows an energy based approach completely designed in the BG domain (Junco, 2004) where: first, the closed-loop specifications are expressed by a so-called Target Bond Graph (TBG), see Figure 2, representing the equivalent closed-loop behavior of the network. Then, in order to obtain the control law, the controlled sources –which provide the manipulated variables in the BG model of the plant– are prototyped (meaning that their behavior is expressed through BG components) in such a way that their power-interconnection with the rest of the plant BG –which is called a Virtual BG (VBG)– matches the TBG. Finally, the control law is obtained from the VBG by simply reading the outputs of the prototyped sources with the help of the causal assignment in the VBG is expressed in (4) for the i^{th} vehicle (an analogous law can be derived for the j^{th} vehicle).

In the vector BG of Figure 2 the corresponding *effort* and *flow* of each bond are vectors of two components each.

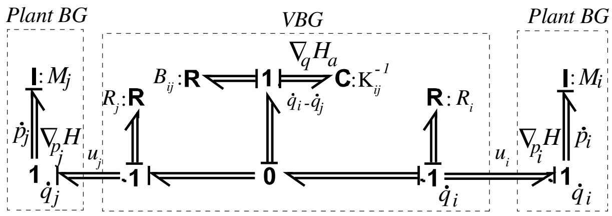

Figure 2: VBG of the interconnection between agents.

$$u_i = -\underbrace{K_{ij}(q_i - q_j - L_{ij})}_{\frac{\partial H_a}{\partial \tilde{q}_{ij}}} - B_{ij}\underbrace{(\dot{q}_i - \dot{q}_j)}_{\frac{\partial H}{\partial p_i} - \frac{\partial H}{\partial p_j}} - R_i\dot{q}_i \qquad (4)$$

where, $K_{ij} = diag(k_{ijx}, k_{ijy})$, $B_{ij} = diag(b_{ijx}, b_{ijy})$ and $L_{ij} = [L_{xij} \quad L_{yij}]^T$ is the natural length of the spring and represents the desired distance to be kept between the two vehicles, B_{ij}, R_i and R_j are design parameters to be chosen. Note that, besides the virtual spring-damper interconnection between the two vehicles, dissipation has been assigned to each of them through the elements with coefficients $R_{i,j}$.

ISBN 978-88-85741-31-7; Bruzzone, Dauphin-Tanguy and Junco Eds

Remark 1: notice that, the first term of (4) is associated with the gradient of the added potential energy due to the action of the spring, i.e. $\frac{\partial H_a}{\partial \tilde{q}_{ij}} = K_{ij}\tilde{q}_{ij}$, where $\tilde{q}_{ij} = (q_i - q_j - L_{ij})$ and $H_a(q_i, q_j) = 1/2\tilde{q}_{ij}{}^T K_{ij}\tilde{q}_{ij}$. Without loss of generality a linear constitutive relationship for the spring and the damper has been chosen. A nonlinear constitutive relationship, particularly in the spring, could provide some advantages in the performance of the closed loop. For example, a nonlinear relation may augment the force exponentially when two vehicles are too close.

Remark 2: notice that, if the vehicles move along a straight line, i.e. the workspace $W \subset \mathbb{R}$, then the vector TBG of Figure 2 is reduced to a single bond TBG.

3.1.1. Obtaining the pH system from the BG

The related pH system can be obtained directly from the BG of Figure 2 via following the procedure detailed in (Donaire and Junco, 2009). In particular, in a BG model with all the storage elements in integral causality, as the one shown in Figure 2, the procedure can be summarized as follows:

1. Compute the total energy of the system using the constitutive relationships of the storage elements.

$$H_{dij}(\tilde{q}_{ij}, p_i, p_j) = \frac{1}{2}p_i^T M_i^{-1} p_i + \frac{1}{2}p_j^T M_j^{-1} p_j + \frac{1}{2}\tilde{q}_{ij}^T K_{ij}\tilde{q}_{ij} \tag{5}$$

   The flow or effort variables entering to the storage elements are the time derivatives $\dot{x}$ of the states which in this example are $\dot{x} = [\dot{q} \quad \dot{p}]^T$, while the outputs of the storage elements are the gradient components of the storage elements $\nabla H_{dij} = \left[\left(K_{ij}(q_i - q_j - L_{ij})\right)^T \quad (M_i^{-1}p_i)^T \quad (M_j^{-1}p_j)^T\right]^T$.

2. Compute the structure and dissipation matrixes J and R using the gains of the causal paths between the storage elements, and between the storage and the dissipation elements, respectively.

$$\begin{bmatrix} \dot{\tilde{q}}_{ij} \\ \dot{p}_i \\ \dot{p}_j \end{bmatrix} = \Bigg[\underbrace{\begin{bmatrix} 0_2 & I_2 & -I_2 \\ -I_2 & 0_2 & 0_2 \\ I_2 & 0_2 & 0_2 \end{bmatrix}}_{J} - \underbrace{\begin{bmatrix} 0_2 & 0_2 & 0_2 \\ 0_2 & \multicolumn{2}{c}{R_d} \\ 0_2 & & \end{bmatrix}}_{R}\Bigg] \nabla H_{dij} \tag{6}$$

Where R_d is the $4x4$ matrix

$$R_d = \begin{bmatrix} -(B_{ij} + R_i) & B_{ij} \\ B_{ij} & -(B_{ij} + R_j) \end{bmatrix}$$

Remark 3: The stability properties of the equilibrium point, $(\bar{p}_i, \bar{p}_j, \tilde{q}_{ij}) = ([0,0]^T, [0,0]^T, [0,0]^T)$, of the closed loop system, defined in the TBG of Figure 2, can be analyzed using the energy function (5) as a Lyapunov function candidate and the *LaSalle* invariance principle.

3.2. DBG and DO in the pH framework

This section defines a closed-loop DBG from a behavioral BG model of the desired closed-loop. The output of the closed-loop DBG is a residual signal that indicates the discrepancy between the desired closed-loop dynamics and real one. Then a DO is defined in the pH framework and its output, i.e. the control input v, is used next to design the outer control loop in order to compensate or attenuate the effect of the perturbation.

Thus the perturbed closed-loop systems results from replacing $u = u_{IDA} + v$ on the plant (1), i.e. with $d \neq 0$, and replacing (4) into (1) results in:

$$\begin{bmatrix} \dot{\tilde{q}}_{ij} \\ \dot{p}_i \\ \dot{p}_j \end{bmatrix} = \begin{bmatrix} 0_2 & I_2 & -I_2 \\ -I_2 & \multicolumn{2}{c}{-R_d} \\ I_2 & & \end{bmatrix} \nabla H_{dij} + \begin{bmatrix} 0_2 \\ v_i \\ v_j \end{bmatrix} + \begin{bmatrix} 0_2 \\ d_i \\ d_j \end{bmatrix} \tag{7}$$

3.2.1. Closed-Loop DBG

The closed-loop DBG is constructed from a behavioral BG model of the desired closed-loop model injecting the plant measurements through modulated sources. The residual signal is then obtained by measuring the power co-variables of the modulated sources, and is an indication of the discrepancy between the desired and real perturbed closed-loop dynamics.

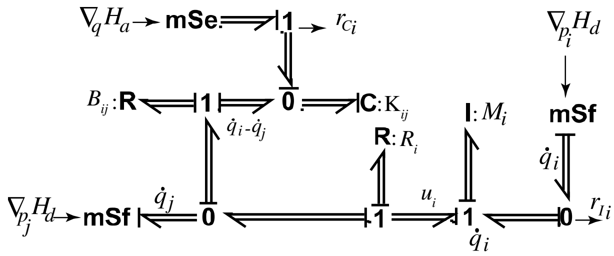

Figure 3: Closed-loop DBG of the interconnection between agents for the i^{th} point mass.

In Figure 3 closed-loop DBG of the interconnection between agents for the i^{th} point mass is shown where the residual signals r_{I_i} and r_{C_i} can be obtained. Notice that, if the masses of the agents are known, then $r_{C_i} = 0$, since the injected effort on the 0-junction is calculated by the control input, i.e. the first term of (4), and $\tilde{q}_{ij}$ is a state of the controller. In addition, the residual signal r_{I_i} can be computed reading the effort on the associated 0-junction as in (9).

Thus replacing the $\dot{p}_i$ of (7) into (9) yields (10), where the residual signal is driven by the perturbations.

$$r_{C_i}(x) = \nabla_{p_i} H_{dij} - \nabla_{p_j} H_{dij} - \dot{\tilde{q}}_{ij} \tag{8}$$

$$r_{I_i}(x) = \dot{p}_i + K_{ij}\tilde{q}_{ij} + B_{ij}(\dot{q}_i - \dot{q}_j) + R_i\dot{q}_i \tag{9}$$

$$r_{I_i}(x) = v_i + d_i \tag{10}$$

The dynamics of the DO for the disturbance is defined using the residual signal as follows.

$$\dot{z}_i = G_i^{-1}\, r_{I_i}(x) \tag{11}$$

Where $G_i > 0, G_i = G_i^T \in R^2$ is a diagonal matrix. Or, expressed in term of the desired closed-loop pH system replacing (9) into (11), yields (12).

$$\dot{z}_i = G_i^{-1}\left[\dot{p}_i + K_{ij}\tilde{q}_{ij} + B_{ij}(\dot{q}_i - \dot{q}_j) + R_i\dot{q}_i\right] \tag{12}$$

To show that z_i is the disturbance estimations replace $\dot{p}_i$ from (7) in (12), with $v_i = -z_i$, obtaining.

$$\dot{z}_i = -G_i^{-1}z_i + G_i^{-1}d_i \tag{13}$$

Then, defining the perturbation error as $e_{d_i} = z_i - d_i$, for $i = 1,2$. and replacing e_{d_i} in (13), the dynamics of e_{d_i} are.

$$\dot{e}_{d_i} = -G_i^{-1}e_{d_i} - \dot{d}_i \tag{14}$$

The perturbation-error dynamics are driven by $\dot{d}_i$, the time derivative of the perturbations. It is straightforward to prove that this error tends to zero exponentially for constant perturbations, i.e. $\dot{d}_i = 0$, and remains bounded if $\|\dot{d}_i\| < \alpha_i$. Notice that the choice of the constant matrix G_i fixes the rate of convergence of the DO.

Remark: the DO defined in (12) depends on the time derivatives of the states, i.e. $\dot{p}_i$. In real applications these variables cannot be always measured via sensors, thus it is needed to compute them with the consequent error due to noise in the measurements. To solve this problem, an internal extra variable of the DO can be defined, see (Mohammadi, Marquez and Tavakoli, 2017) for further details about this procedure. In this example, i.e. two masses connected through the VBG of Figure 2 integrating (12) allows to express the control input $v_i = -z_i$ in terms of the closed loop variable as in (15).

$$\begin{aligned} v_i = &-G_i^{-1}M_i\dot{q}_i - G_i^{-1}B_{ij}(q_i - q_j) - G_i^{-1}R_iq_i \\ &- G_i^{-1}\int_0^t K_{ij}\tilde{q}_{ij}\, d\tau \end{aligned} \tag{15}$$

3.2.2. DO in the pH framework

The previous ideas, elaborated above on the Bond Graph domain for the control of just one vehicle of the platoon, is extended to the whole system and theoretically developed in the pHs set-up, for further details on this approach refer to (Nacusse, Donaire and Junco, 2018) . Figure 4 depicts the block diagram representation of the connection between the plant and the so-called Diagnostic pH system (D-pH), where the measurements injected into the D-pH block are identified as the gradient of the Hamiltonian or stored energy.

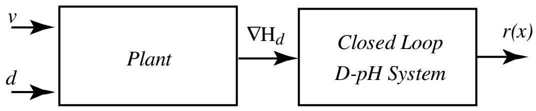

Figure 4: Interconnection between plant and Closed-loop D-pH System.

Figure 5 shows an internal representation of the D-pH system, where it is assumed that ∇H_d is bijective, i.e. exists $h_d(\nabla H_d(x)) = x$. Notice that, x is the state variable driven by the dynamics of the perturbed system. Where $J_d(x)$ and $R_d(x)$ are the desired interconnection and dissipation matrices.

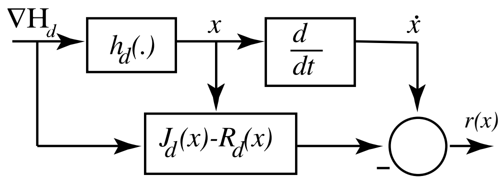

Figure 5: Internal block diagram of the closed-loop D-pH.

The system (16) represents the closed-loop system with the control input $u = u_{IDA} + v$, being u_{IDA} the collection of all interconnection control laws of the form (4).

$$\begin{aligned} \begin{bmatrix}\dot{\tilde{q}} \\ \dot{p}\end{bmatrix} &= \begin{bmatrix} 0_m & S \\ -S^T & -R_d \end{bmatrix}\begin{bmatrix}\nabla_{\tilde{q}}H_d \\ \nabla_p H_d\end{bmatrix} + \begin{bmatrix}0 \\ I\end{bmatrix}(v + d) \\ y &= \nabla_p H \end{aligned} \tag{16}$$

With $H_d(\tilde{q}, p) = \frac{1}{2}p^T\mathcal{M}^{-1}p + \frac{1}{2}\tilde{q}^T K\tilde{q}$

Where $p \in R^{2N}$ and $\tilde{q} \in R^m$ are column vectors that collect all the generalized momenta of the vehicles masses and the states of the springs, respectively. S is a $mx2N$ matrix with most of its elements equal to zero and that contains only a 1 and a -1 on each row representing the interconnection structure between agents; R_d is the dissipation structure matrix, which is assumed positive definite by design; $\mathcal{M} = diag(M_1, \dots, M_N)$ and $K = diag(K_1, \dots, K_m)$.

Thus, the outputs of the D-pH are $r(x) = [r_q(x), r_p(x)]^T$:

$$r_q(x) = \dot{\tilde{q}} - S\nabla_p H_d \tag{17}$$

$$r_p(x) = \dot{p} + S^T \nabla_{\tilde{q}} H_d + R_d \nabla_p H_d \quad (18)$$

The same procedure described above in the BG domain can be applied to (18) to obtain the output of the DO.

$$\dot{z} = G^{-1}\, r_p(x) \quad (19)$$

$$\dot{z} = -G^{-1}\, z + G^{-1} d \quad (20)$$

where $G = diag(G_1, \dots, G_N)$ is the gain of the DO.

4. MAIN RESULT

In this section the properties of a network of N interconnected agents, with an extra control law v which depends on the output of the DO, are studied. The network of N interconnected agents is represented by the system (16) where each agent can be coupled to more than one neighbor depending on the network configuration.

Proposition:

System (16) with the disturbance estimation z (19) and control input (20) has the following properties:

$$v = -z - \left(\frac{1}{4}\right) GG^T \nabla_p H_d \quad (21)$$

1- It can be expressed as a pH system as:

$$\begin{bmatrix} \dot{\tilde{q}} \\ \dot{p} \\ \dot{z} \end{bmatrix} = [J_c - R_c] \nabla Q + \beta\, d \quad (22)$$

With $J_c = \begin{bmatrix} 0 & S & 0 \\ -S^T & 0 & -\frac{1}{2}G \\ 0 & \frac{1}{2}G^T & 0 \end{bmatrix}, R_c = \begin{bmatrix} 0 & 0 & 0 \\ 0 & R_d^* & \frac{1}{2}G \\ 0 & \frac{1}{2}G^T & I \end{bmatrix}$, $R_d^* = R_d + \left(\frac{1}{4}\right) GG^T$, $\beta = [0 \quad I \quad G^{-1}]^T$ *and* $Q(p, \tilde{q}, z) = H_d(p, \tilde{q}) + \frac{1}{2} z^T G^{-1} z$*:* where the 0 and I are the zero and identity matrices with appropriate dimensions.

2- If the disturbance d is constant, that is $d(t) = d_c$ and $d_d(t) = 0$, then the equilibrium $(p^*, \tilde{q}^*, z^*) = (0, 0, d_c)$ of the closed loop is asymptotically stable with Lyapunov function (23):

$$Q_2 = H_d(p, \tilde{q}) + \frac{1}{2}(z - d_c)^T G^{-1} (z - d_c) \quad (23)$$

3- The closed loop system (22) is l_2 weakly string stable with respect to the dynamic disturbances $d(t)$.

Notice that the term $(1/4) GG^T \nabla_p H_d$ in (21) is a damping that always can be injected.

Proof:

1- To prove the first claim consider $Q(p, \tilde{q}, z) = H_d(p, \tilde{q}) + \frac{1}{2} z^T G^{-1} z$, then writing the dynamics of the states $[p, \tilde{q}]$ and substituting the input by the control law (21), yields the closed loop dynamics (24):

$$\begin{bmatrix} \dot{\tilde{q}} \\ \dot{p} \\ \dot{z} \end{bmatrix} = \begin{bmatrix} 0 & S & 0 \\ -S^T & -R_d^* & -G \\ 0 & 0 & -I \end{bmatrix} \begin{bmatrix} \nabla_{\tilde{q}} H_d \\ \nabla_p H_d \\ G^{-1} z \end{bmatrix} + \begin{bmatrix} 0 \\ 1 \\ -G^{-1} \end{bmatrix} d \quad (24)$$

Finally decompose the matrix that multiplies ∇Q in (24) into its symmetric and skew-symmetric component to obtain the dynamics (22).

2- To prove that $(p^*, \tilde{q}^*, z^*) = (0, 0, d_c)$ is an asymptotically stable equilibrium point of the system define Q_2 as in (23), then the closed loop system can be expressed as:

$$\begin{bmatrix} \dot{\tilde{q}} \\ \dot{p} \\ \dot{z} \end{bmatrix} = [J_c - R_c] \nabla Q_2 \quad (25)$$

Use Q_2 as a candidate Lyapunov function, and compute its time derivative, which result as follows

$$\dot{Q}_2 = \nabla {Q_2}^T \begin{bmatrix} \dot{\tilde{q}} \\ \dot{p} \\ \dot{z} \end{bmatrix} \quad (26)$$

$$\dot{Q}_2 = \nabla {Q_2}^T \begin{bmatrix} 0 & S & 0 \\ -S^T & -R_d^* & -G \\ 0 & 0 & -I \end{bmatrix} \nabla Q_2 \quad (27)$$

$$\dot{Q}_2 = -\nabla {Q_2}^T \begin{bmatrix} 0 & 0 & 0 \\ 0 & R_d^* & \frac{1}{2}G \\ 0 & \frac{1}{2}G^T & I \end{bmatrix} \nabla Q_2 \quad (28)$$

$$\dot{Q}_2 = \begin{bmatrix} \nabla_p H_d \\ G^{-1}(z - d_c) \end{bmatrix}^T \underbrace{\begin{bmatrix} R_d^* & \frac{1}{2}G \\ \frac{1}{2}G^T & I \end{bmatrix}}_{R_c^*} \begin{bmatrix} \nabla_p H_d \\ G^{-1}(z - d_c) \end{bmatrix} \quad (29)$$

Applying Schur's complements in $R_c^* > 0 \Leftrightarrow R_d^* > 0$ which implies that $\dot{Q}_2 \leq 0$. Thus, the equilibrium point is asymptotically stable via the application of the *La Salle* Invariance Principle, which ensures that the trajectories of the state converge to the largest invariant set (Khalil, 2002).

3- The procedure used to prove *Theorem 4* in (Knorn et al., 2014) it is used here to prove this claim. Using $H_d(p,\tilde{q})$ as candidate of Lyapunov function and following the procedure of the proof of the claim 2, then the derivative of $H_d(p,\tilde{q})$ along the trajectories can be written as:

$$\dot{\mathrm{H}}_\mathrm{d} \leq -\nabla \mathrm{H_d}^\mathrm{T} \begin{bmatrix} 0 & 0 & 0 \\ 0 & R_d^* & \frac{1}{2}\mathrm{G} \\ 0 & \frac{1}{2}\mathrm{G}^\mathrm{T} & I \end{bmatrix} \nabla \mathrm{H_d} + \nabla \mathrm{H_d}^\mathrm{T} d_d \tag{30}$$

$$\dot{\mathrm{H}}_\mathrm{d} \leq -\chi^T \begin{bmatrix} R_d^* & \frac{1}{2}\mathrm{G}^\mathrm{T} \\ \frac{1}{2}G^T & I \end{bmatrix} \chi + \chi^T \delta_d \tag{31}$$

where $\chi = \begin{bmatrix} \nabla_p H_d & G^{-1}z \end{bmatrix}$ and $\delta_d = \begin{bmatrix} I \\ G^{-1} \end{bmatrix} d_d$ then:

$$\dot{\mathrm{H}}_\mathrm{d} \leq -\lambda_{min}(R_d^*)|\chi|^2 + \chi^T \delta_d \tag{32}$$

$$\dot{\mathrm{H}}_\mathrm{d} \leq -\frac{1}{2}\lambda_{min}(R_d^*)|\chi|^2 + \frac{1}{2\lambda_{min}(R_d^*)}|\delta_d|^2 \tag{33}$$

$$\dot{\mathrm{H}}_\mathrm{d} \leq \frac{1}{2\lambda_{min}(R_d^*)}|\delta_d|^2 \tag{34}$$

Then, integrating both terms of (34) along time:

$$\mathrm{H_d}(t) \leq \mathrm{H_d}(0) + \frac{1}{2\lambda_{min}(R_d^*)}\|\delta_\mathrm{d}\|_2{}^2 \tag{35}$$

Replacing $H_d(0)$ and operating yields

$$\begin{aligned} H_d(t) \leq & \frac{1}{2}\lambda_{min}(M^{-1})|p(0)| + \frac{1}{2}\lambda_{min}(K)|\tilde{q}(0)| \\ & + \frac{1}{2}\lambda_{min}(G^{-1})|z(0)| + \frac{1}{2\,\lambda_{min}(R_d^*)}\|\delta_d\|_2{}^2 \end{aligned} \tag{36}$$

Which means that $\mathrm{H_d}(p,\tilde{\mathrm{q}},z,t)$ is bounded for all agents if $|p(0)|$, $|\tilde{q}(0)|$, $|z(0)|$, and $\|\delta_d\|^2$ do not increase with number of agents N. As $H_d(p,q,z,t)$ is monotically increasing, then an upper bound of $\mathrm{H_d}(p,\tilde{\mathrm{q}},z,t)$ implies that the states $(p,\tilde{q},z)$ are also bounded. Therefore, the system is l_2 weakly string stable with respect to the dynamic disturbances $d_d(t)$.

5. APPLICATION EXAMPLES

This section presents some simulations results to show the performance of the control laws obtained above in two different configurations among agents. First a *partially coupled network* is studied, see Figure 6a, in which each agent has coupling index $k = 2$, i.e. each agent is connected to only two other agents, and then a *fully coupled network*, see Figure 6b, configuration in which the agents are connected to all the surrounding agents with distance $D_i \leq 2$.

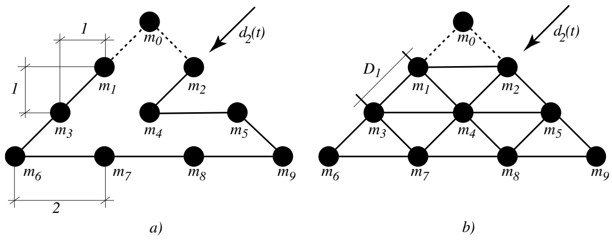

Figure 6: Interconnection and distance, in meters, among agents. a) *partially coupled network* with coupling index $k = 2$. b) *fully coupled network.*

Figure 6 shows the desired triangle formation where the black dots represent the agents and the connections among them are represented by lines. The dashed lines represent the unidirectional coupling of *agent 1* and *agent 2* with the leader, while the solid lines represent the bi-directional coupling among agents, i.e. in the BG domain these lines are represented with the VBG shown in Figure 2.

The simulations were performed using 20sim environment (20Sim, 2013) and the scenario is as follows: at time $t = 0sec$ the agents are gathered at the origin and then they move to the desired triangle formation. At time $t = 8sec$ the leader moves 1 meter in the Y direction. Finally, at time $t = 20sec$ a disturbance, which is a logarithmic sine sweep of the form, $d(t) = 50\sin(\omega(t)t)$ (see 20Sim reference manual for further details), affects the agent 2 as indicated in Figure 6.

The parameters used in the simulations are: $m_i = 1Kg$, for $i = 0\ to\ 9$, $B_i = 0\,I_2Kg/sec$, $B_{ij} = 10I_2Kg/sec$, $K_{ij} = 10I_2Kg/sec^2$, $L_{ij} = I_2m$ and $G_i = 100I_2$, where I_2 is the $2x2$ identity matrix.

In Figure 7 the position of the leader, the disturbance affecting the mass 2 and the disturbance error are depicted for both configurations. Notice that the disturbance error can be reduced even more by increasing the value of G_i.

Figure 8 and Figure 9 show the distance between the leader and each agent for the *partially coupled network* and the *fully coupled network* configuration respectively, with and without the action of the DO. The distance between the leader and each agent, defined in the desired formation configuration of Figure 6, is $Dist\_m_i = |q_0 - q_i|$ for $i = 0\ to\ 9$. As can be seen in Figure 8a and Figure 9a for time $t < 20\,sec$ and in Figure 8b and Figure 9b the $Dist\_m_i$ of each agent reaches the desired distance. Notice, the improvement due to the application of the control input v in Figure 8b and Figure 9b for time $t > 20\ sec$.

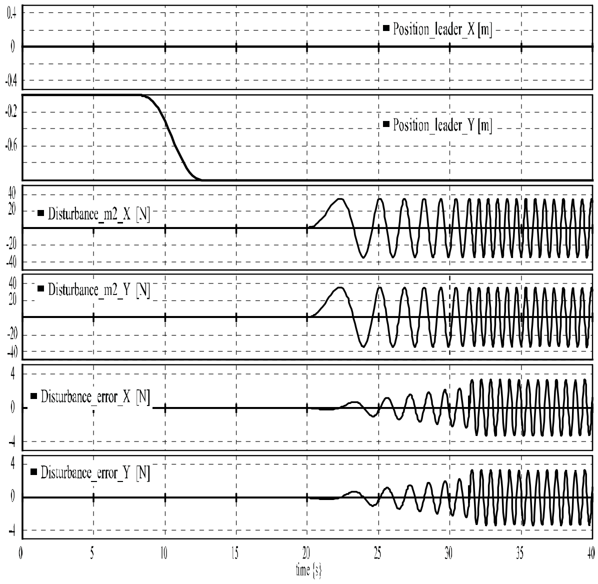

Figure 7: From top to bottom: Cartesian position XY of the leader; Cartesian disturbance XY acting on m_2; Cartesian disturbance errror XY obtained from the DO.

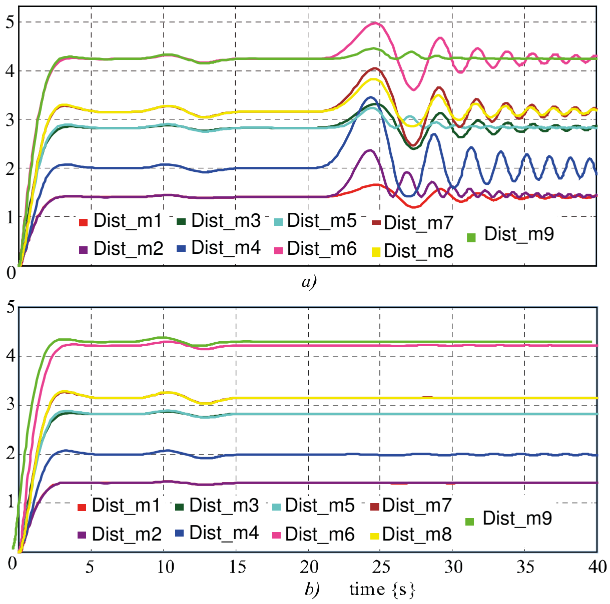

Figure 8: Distance, in meters, between the leader and each agent. a) without DO compensator, b) with DO compensator.

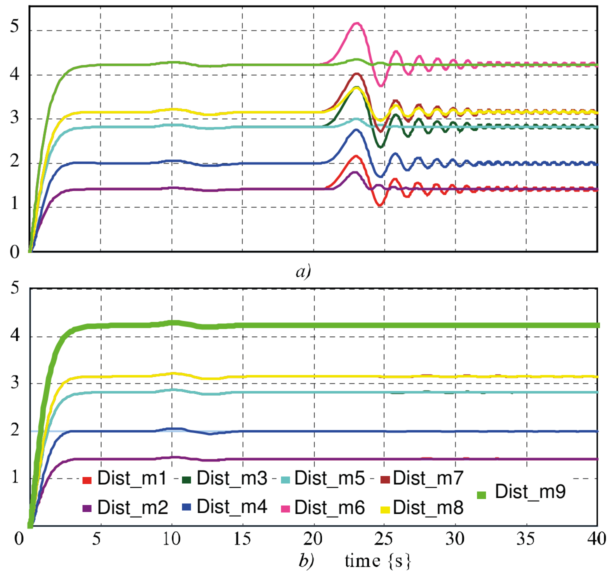

Figure 9: Distance, in meters, between the leader and each agent. a) without DO compensator, b) with DO compensator.

6. CONCLUSIONS

This work tackles the problem of formation control for a group of holonomic vehicles using the Bond Graphs formalism. The control laws for the agents are physically inspired and designed in the BG domain. Later these control laws are robustified by adding an extra control action based in a DO definition. The main properties of the resulting closed-loop are: constant disturbance rejection and l_2 weakly string stable with respect to disturbances.

ACKNOWLEDGMENTS

The authors wish to thanks SeCyT-UNR (the Secretary for Science and Technology of the National University of Rosario) for their financial support through project PID-UNR 1ING502 and the ANPCyT (Argentine National Agency for Scientific and Technological Promotion), under project PICT 2017-3644.

APPENDIX

The perturbed TBG for *partially coupled network* and the *fully coupled network* interconnection are shown in Figure 10 and Figure 11, where the interconnection between the 1-junctions in done through the VBG of Figure 2. The matrixes S and R of the system (16), are not deduced here due to space constraint, but these can be computed following the procedure detailed in Section 3.1.1.

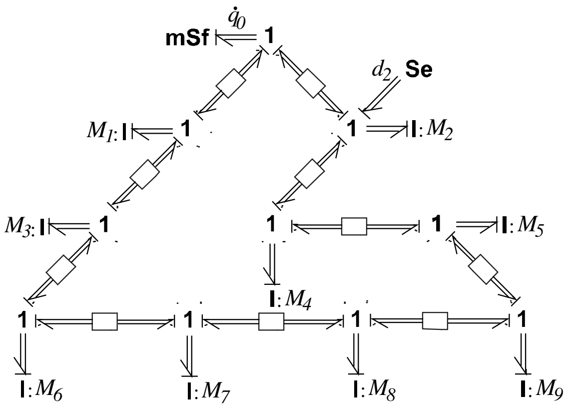

Figure 10: Perturbed TBG of 10 agents in triangle formation for *partially coupled network* of Figure 6a.

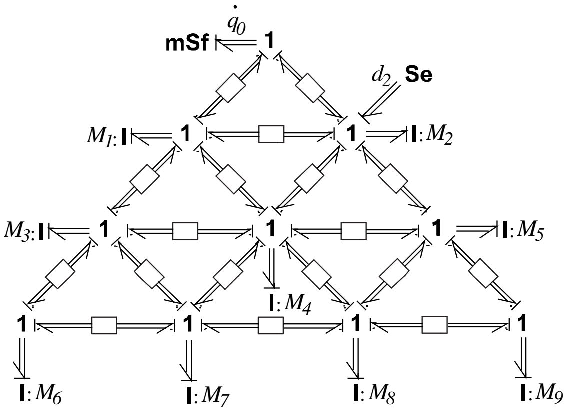

Figure 11: Perturbed TBG of 10 agents in triangle formation for *partially coupled network* of Figure 6b.

REFERENCES

20Sim (2013) *Controllab Products, B. V.*, Available: http://www.20sim.com.

Arcak, M. (2007) 'Passivity as a Design Tool for Group Coordination', *IEEE Transactions on Automatic Control*, vol. 52, no. 8, Aug, pp. 1380-1390.

Barooah, P., Mehta, P.G. and Hespanha, J.P. (2009) 'Mistuning-Based Control Design to Improve Closed-Loop Stability Margin of Vehicular Platoons', *IEEE Transactions on Automatic Control*, vol. 54, no. 9, Sep., pp. 2100-2113.

Donaire, A. and Junco, S. (2009) 'Derivation of input-state-output port-hamiltonian systems from bond graphs', *Simulation Modelling Practice and Theory*, vol. 17, no. 1, pp. 137-151.

Donaire, A. and Junco, S. (2009) 'Energy shaping, interconnection and damping assignment, and integral control in the bond graph domain', *Simulation Modelling Practice and Theory*, vol. 17, no. 1, pp. 152-174.

Feddema, J.T., Lewis, C. and Schoenwald, D.A. (2002) 'Decentralized control of cooperative robotic vehicles: theory and application', *IEEE Transactions on Robotics and Automation*, vol. 18, no. 5, Oct, pp. 852-864.

Galceran, E. and Carreras, M. (2013) 'Planning coverage paths on bathymetric maps for in-detail inspection of the ocean floor', 2013 IEEE International Conference on Robotics and Automation, 4159-4164.

Gao, W., Jiang, Z., Lewis, F.L. and Wang, Y. (2018) 'Leader-to-Formation Stability of Multiagent Systems: An Adaptive Optimal Control Approach', *IEEE Transactions on Automatic Control*, vol. 63, no. 10, Oct, pp. 3581-3587.

Hameed, I.A. (2014) 'Intelligent Coverage Path Planning for Agricultural Robots and Autonomous Machines on Three-Dimensional Terrain', *Journal of Intelligent Robotic Systems*, vol. 74, no. 3, Jun, pp. 965-983.

Ji, W., Li, J.L., Zhao, D.A. and Jun, Y. (2014) 'Obstacle Avoidance Path Planning for Harvesting Robot Manipulator Based on MAKLINK Graph and Improved Ant Colony Algorithm', Advances in Measurements and Information Technologies, 1063-1067.

Junco, S. (2004) 'Virtual Prototyping of Bond Graphs Models for Controller Synthesis through Energy and Power Shaping', International Conference on Integrated Modeling and Analysis in Applied Control and Automation (IMAACA 2004).

Karnopp, D.C., Margolis, D.L. and Rosenberg, R.C. (2006) *System Dynamics: Modeling and Simulation of Mechatronic Systems*, New York, NY, USA: John Wiley \& Sons, Inc.

Khalil, H.K. (2002) *Nonlinear Systems*, Prentice Hall PTR.

Knorn, S., Donaire, A., Agüero, J.C. and Middleton, R.H. (2014) 'Passivity-based control for multi-vehicle systems subject to string constraints', *Automatica*, vol. 50, no. 12, pp. 3224-3230.

Knorn, S. and Middleton, R.H. (2013) 'Two-dimensional analysis of string stability of nonlinear vehicle strings', 52nd IEEE Conference on Decision and Control, 5864-5869.

Middleton, R.H. and Braslavsky, J.H. (2010) 'String Instability in Classes of Linear Time Invariant Formation Control With Limited Communication Range', *IEEE Transactions on Automatic Control*, vol. 55, no. 7, July, pp. 1519-1530.

Mohammadi, A., Marquez, H.J. and Tavakoli, M. (2017) 'Nonlinear Disturbance Observers: Design and Applications to Euler-Lagrange Systems', *IEEE Control Systems*, vol. 37, Aug, pp. 50-72, Available: ISSN: 1066-033X.

Nacusse, M., Donaire, A. and Junco, S. (2018) 'Robustifying Passive Closed-Lopp Port-Hamiltonian Systems Using Observer Based Control', International Conference on Integrated Modeling and Analysis in Applied Control and Automation (IMAACA 2018).

Nacusse, M. and Junco, S. (2011) 'Passive Fault Tolerant Ccontrol: a Bond Graph Approach', International Conference on Integrated Modeling and Analysis in Applied Control and Automation (IMAACA 2011).

Nacusse, M. and Junco, S. (2015) 'Bond-graph-based controller design for the quadruple-tank process', *International Journal of Simulation and Process Modelling.*, vol. 10, pp. 179-191.

Ollero, A., Marron, P.J., Bernard, M., Lepley, J., la Civita, M., de Andres, E. and van Hoesel, L. (2007) 'AWARE: Platform for Autonomous self-deploying and operation of Wireless sensor-actuator networks cooperating with unmanned AeRial vehiclEs', 2007 IEEE International Workshop on Safety, Security and Rescue Robotics, 1-6.

Ortega, R. and García-Canseco, E. (2004) 'Interconnection and Damping Assignment Passivity-Based Control: A Survey', *European Journal of Control*, vol. 10, no. 5, pp. 432-450.

Radke, A. and Gao, Z. (2006) 'A survey of state and disturbance observers for practitioners', 2006 American Control Conference, 6 pp.-.

Samantaray, A.K., Medjaher, K., Bouamama, B.O., Staroswiecki, M. and Dauphin-Tanguy, G. (2006) 'Diagnostic bond graphs for online fault detection and isolation', *Simulation Modelling Practice and Theory*, vol. 14, no. 3, pp. 237-262.

Seiler, P., Pant, A. and Hedrick, K. (2004) 'Disturbance propagation in vehicle strings', *IEEE Transactions on Automatic Control*, vol. 49, no. 10, Oct, pp. 1835-1842.

Soni, A. and Hu, H. (2018) 'Formation Control for a Fleet of Autonomous Ground Vehicles: A Survey', *Robotics*, vol. 7, no. 4.

Swaroop, D. and Hedrick, J.K. (1996) 'String stability of interconnected systems', *IEEE Transactions on Automatic Control*, vol. 41, no. 3, March, pp. 349-357.

Swaroop, D. and Hedrick, J. (1999) 'Constant Spacing Strategies for Platooning in Automated Highway Systems.', *ASME. J. Dyn. Sys., Meas., Control.*, vol. 121, no. 3, pp. :462-470.

Tuna, G., Gungor, V.C. and Gulez, K. (2014) 'An autonomous wireless sensor network deployment system using mobile robots for human existence detection in case of disasters', *Ad Hoc Networks*, vol. 13, pp. 54-68.

Tuna, G., Güngör, V.Ç. and Potirakis, S.M. (2015) 'Wireless sensor network-based communication for cooperative simultaneous localization and mapping', *Computers \& Electrical Engineering*, vol. 41, pp. 407-425.

Xiao, L., Gao, F. and Wang, J. (2009) 'On scalability of platoon of automated vehicles for leader-predecessor information framework', 2009 IEEE Intelligent Vehicles Symposium, 1103-1108.

Yuming, L., Ruchun, W., Zhenli, Z. and Junlin, Z. (2011) 'Dynamic coverage path planning and obstacle avoidance for cleaning robot based on behavior', 2011 International Conference on Electric Information and Control Engineering, 4952-4956.

Zheng, Y., Eben Li, S., Wang, J., Cao, D. and Li, K. (2016) 'Stability and Scalability of Homogeneous Vehicular Platoon: Study on the Influence of Information Flow Topologies', *IEEE Transactions on Intelligent Transportation Systems*, vol. 17, no. 1, Jan, pp. 14-26.